Available online at www.sciencedirect.com
SCIENCE DIRECT®
Journal of Power Sources 127 (2004) 58–64
JOURNAL OF POWER SOURCES
www.elsevier.com/locate/jpowsour

Aging mechanisms of lithium cathode materials

M. Wohlfahrt-Mehrens*, C. Vogler, J. Garche

ZSW Center for Solar Energy and Hydrogen Research, Baden Wuerttemberg, Division 3, Electrochemical Energy Storage and Conversion, Helmholtzstraße 8, Ulm D-89081, Germany

Abstract

Batteries for stationary and automotive applications are required to provide extended cycle life and calendar life. Lithium–manganese oxides ($LiMn_2O_4$) with spinel structure and lithium–nickel–cobalt mixed oxides ($LiNiCoO_2$) with layered structures have been extensively studied in the last few years for usage in high energy and high power batteries in order to replace lithium–cobalt oxide ($LiCoO_2$) as cathode material in terms of cost, abundance and performance. In this paper, we summarize some basic mechanisms responsible for capacity fading under cycling and different storage conditions for both types of cathode materials. Lithium–nickel–cobalt mixed oxides show excellent storage stability in the discharged state and low metal solubility in the electrolyte. The cycling stability is mainly influenced by structural changes in the delithiated state and thermal instability arises from oxygen release at elevated temperatures in the charged state. Small amounts of aluminum and magnesium dopants stabilize the layered structure and increase cycling stability of lithium–nickel–cobalt oxide. Different mechanisms of capacity fading especially at higher temperatures are discussed for lithium–manganese oxide spinels. Capacity fading is highly dependent on cycling and storage conditions and caused by structural changes as well as by side reactions with electrolyte catalyzed by decomposition products of $LiPF_6$ conducting salt and H_2O impurities in the electrolyte.

Keywords: Lithium–nickel–cobalt oxide; Lithium–manganese spinel; Calendar life; Capacity fading; Aging mechanism

1. Introduction

Lithium ion batteries are attractive candidates for automotive applications due to their high energy and power density. These applications require both extended cycle life and prolonged calendar life. For that reason, estimation and prediction of battery lifetime, as well as capacity fading mechanisms and their prevention, are of increasing interest. General test procedures are required, which enable the extrapolation of battery lifetime under realistic conditions. These techniques have to be developed exclusively for each cell design and cell chemistry. Some studies on aging of lithium ion batteries have been published in the last years [1,2].

A number of changes in the lithium ion cell may influence the lifetime of the lithium ion cell:

- Degradation of active materials.
- Degradation or changes of electrode compounds like conducting agents, binder, and current collector.
- Decomposition and film formation of electrolytes.

These effects do not occur separately and cannot be discussed independently from each other. They depend sensitively on individual cell chemistry and cell design as well as performance data and will vary from battery manufacturer to battery manufacturer.

This paper focuses on the description of some basic capacity fading mechanisms based on positive active materials from literature data and emphasizes differences between lithium–nickel–cobalt mixed oxide and lithium–manganese spinel, which are currently the most suitable cathode materials for automotive applications.

2. Experimental

Lithium–nickel–cobalt mixed oxides have been synthesized by mixing stoichiometric amounts of lithium compound with a mixed nickel–cobalt compound and Mg- or Al-containing compound followed by heat treatment. Precursors for mixed doped spinel samples have been prepared by solution precipitation technique. Heat treatment of the precursors lead to doped $LiMn_2O_4$. Further details are described elsewhere [3].

Composition of lithium metal oxides and dissolution of cobalt, nickel and manganese have been analyzed by ICP

* Corresponding author. Tel.: +49-731-9530-601; fax: +49-731-9530-666.
E-mail address: margret.wohlfahrt-mehrens@zsw-bw.de (M. Wohlfahrt-Mehrens).

0378-7753/$ – see front matter © 2003 Elsevier B.V. All rights reserved.
doi:10.1016/j.jpowsour.2003.09.034

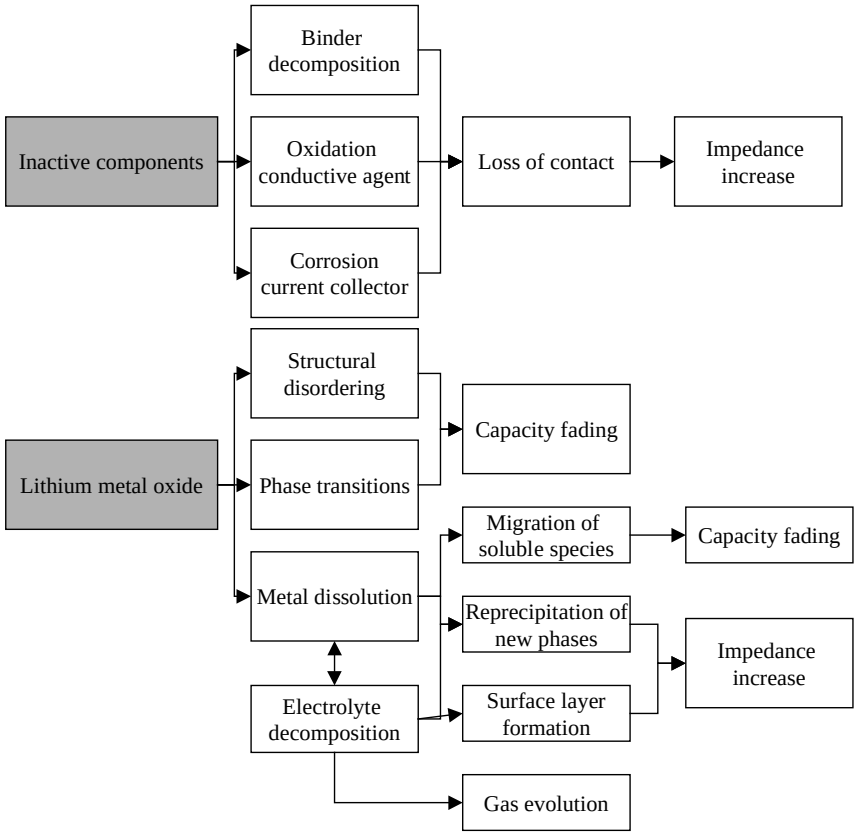

Fig. 1. Schematic overview on basic aging mechanisms of cathode materials.

analysis. X-ray diffraction profiles of powders and electrodes have been measured with Siemens D5000 diffractometer (Cu Kα radiation, graphite secondary monochromator).

2.1. General aspects of capacity fading at positives

In general, capacity fading of positive active material can originate from three basic principles:

- Structural changes during cycling.
- Chemical decomposition/dissolution reaction.
- Surface modification.

In contrast to the negative carbon material, degradation of positive active material is dependent on state of charge (SoC) and cycling conditions. The electrochemical reaction of the positive proceeds as an intercalation reaction of lithium ions in the metal oxide:

$$\mathrm{LiMeO_2} \rightleftarrows \mathrm{Li}_x\mathrm{MeO_2} + (1-x)\mathrm{Li}^+ + (1-x)\mathrm{e}^-$$

The insertion/extraction of lithium ions leads to changes in the molar volume of the materials, which may induce mechanical stress and strain to the electrode. Also, phase transitions can occur which lead to distortion of the crystal lattice and further mechanical stress.

In order to obtain high cycle life these effects have to be minimized by optimizing the composition and structure of the cathode material. Fig. 1 gives a schematic overview on aging mechanisms for lithium ion cathode materials, which have been described in literature, so far.

3. Lithium–nickel–cobalt oxides

3.1. Structural aspects

Lithium–nickel–cobalt mixed oxides provide high specific capacity and good cycling stability. $LiNiO_2$ and $LiCoO_2$ are end members of a complete homogeneous solid solution series and are crystallized in the α-$NaFeO_2$ structure pure lithium–nickel oxide exhibit a number of reversible phase transitions during electrochemical lithiation/delithiation [4–13]. Fig. 2 gives the phase domains in Li_xNiO_2. The transition of the monoclinic phase domain M1 and the formation of the totally delithiated phase H3 lead to large and anisotropic volume jumps and as a result to a rapid decrease in capacity. The monoclinic transition can be prevented by cobalt content of about 20 mol%. Aluminum and magnesium dopants lead to further stabilization of the layered structure. The total volume changes of lithium–nickel–cobalt oxide are rather low [14] and can be minimized by additional doping with aluminum [15–17] or magnesium [18,19]. Therefore, Al- or Mg-doped lithium–nickel–cobalt oxides exhibit better cycle life compared to undoped materials (Fig. 3).

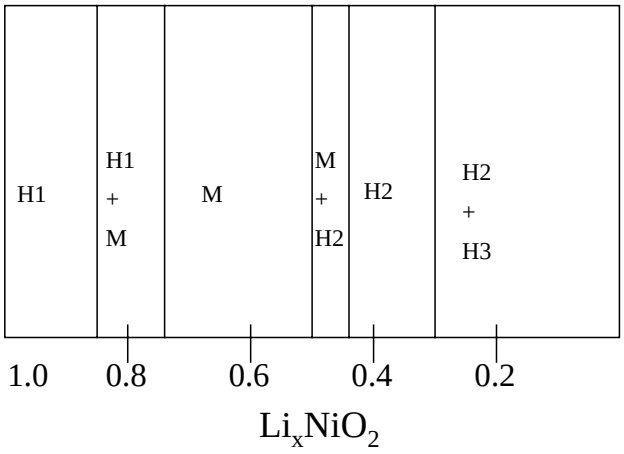

Fig. 2. Phase diagram for Li_xNiO_2. H1: hexagonal phase 1, M: monoclinic phase, H2: hexagonal phase 2, H3: hexagonal phase 3.

However, structural changes in $Li_x(Ni, Co)O_2$ still occur for $x < 0.25$. The two-phase reaction in the upper potential formation is still present. There are also indications that nickel cations slowly migrate into the delithiated lithium layers of the host structure, if the electrode is overcharged. The formation of the fully delithiated phase, however, can only be prevented by a careful limitation of the end-of-charge voltage. Thereby, maximal 75% of the theoretical capacity of lithium–nickel–cobalt oxide are usable.

$Li(Ni, Co)O_2$ with optimized composition is very stable in the discharged state even at higher temperatures and exhibit very good cycle life, if the end-of-charge voltage is controlled carefully and overcharge can be avoided.

3.2. Dissolution

The dissolution of lithium–nickel–cobalt mixed oxide in practical electrolytes is very low. After 4-week storage of $LiNi_{0.8}Co_{0.15}Al_{0.05}O_2$ in 1 M $LiPF_6$ in EC/DMC at 40 °C, the amount of cobalt and nickel in the electrolyte was below the limit of detection. Dissolution of lithium–nickel–cobalt oxide in practical electrolytes does only occur under extreme conditions.

3.3. Surface effects

Surface–electrolyte interactions and formation of surface layers (SEI) have been widely investigated and described for anode materials of lithium ion batteries [20,21]. According to Broussely et al., the increase of interfacial impedance of the carbon anode is responsible for the power fading of high power batteries [2]. However, in some other works, increase of interfacial impedance is also observed for the positive electrode of high power batteries [22–27]. Lithium–nickel–cobalt oxide often shows an increase of impedance during extended cycling or storage. This increase is accelerated by higher temperature and by high end-of-charge voltages above 4.2 V versus Li/Li^+.

3.4. Conclusions

Capacity fading caused by structural changes can be minimized by adjusting composition of active material and controlling the end-of-charge voltage. In general, electrode aging is accelerated by high ΔSoC and high cycling rates. Both phase transitions and formation of surface films occur only at high state of charge and at high potentials and are accelerated by higher temperatures.

4. Lithium–manganese spinel

The capacity fading mechanisms are more complex, if $LiMn_2O_4$ is used as positive material. Cycle life and calendar life are strongly dependent on both the composition of active material and state of charge. The mechanisms are not fully

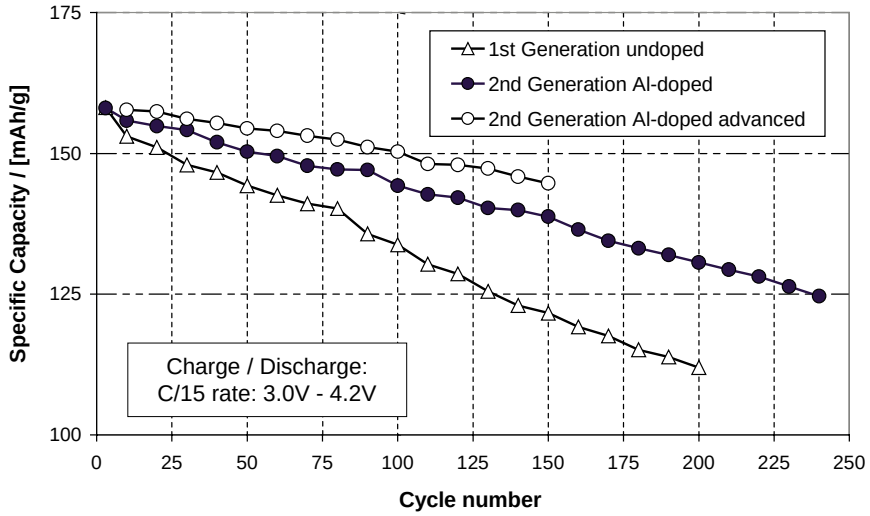

Fig. 3. Cycle life of doped lithium–nickel–cobalt oxides.

clarified yet but can roughly classified as follows:

- Changes at low SoC (discharged state):
  - Structural changes due to Jahn–Teller distortion of Mn^{3+} [28,29].
  - Decomposition reaction and dissolution of Mn^{2+} in electrolyte.
- Changes at high SoC (charged state):
  - Thermodynamic instability of delithiated lithium–manganese spinel.
  - Electrolyte oxidation [30,31].
  - Formation of an oxygen-rich spinel [32].
  - Site exchange between Li and Mn [33].

4.1. Structural aspects

The electrode reaction of lithium–manganese spinel is given by: $LiMn_2O_4 \rightarrow Li_xMn_2O_4 + (1-x)Li^+ + (1-x)e^-$. At low potentials, lithium–manganese spinel can insert additional lithium and a Mn(III) Jahn–Teller distorted tetragonal phase is formed.

Fig. 4 shows a typical potential–composition curve of $Li_xMn_2O_4$. The correlation between potential plateau and structural changes has been investigated extensively by X-ray diffraction methods [34–38]. A phase transition occurs at $x = 0.5$, which is explained by formation of an ordered lithium superstructure. In recent studies [39–41], further phase transitions have been identified for stoichiometric lithium–manganese oxides.

In order to obtain good cycling stability, the formation of the lithium superstructure phase at $x = 0.5$ [42] and the formation of the double hexagonal phase [43] have to be prevented.

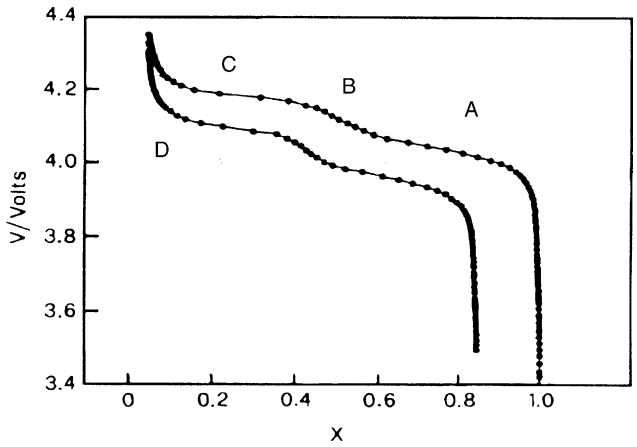

Fig. 4. Potential of a lithium–manganese spinel electrode vs. Li/Li^+ in dependence on x in $Li_xMn_2O_4$.

Improvement of capacity retention has been achieved by two ways:

- partial substitution of manganese ions by trivalent or divalent cations like Co, Cr, Al and Mg [44–47];
- partial substitution of manganese by excess lithium [48–54].

Both strategies lead to:

- decrease of Mn(III) content ⇒ improved stability in the discharged state;
- fixing of lithium in the host lattice ⇒ improved stability in the charged state;
- decrease of volume changes during cycling ⇒ improved cycling stability;
- prevention of formation of super structures ⇒ improved cycling stability.

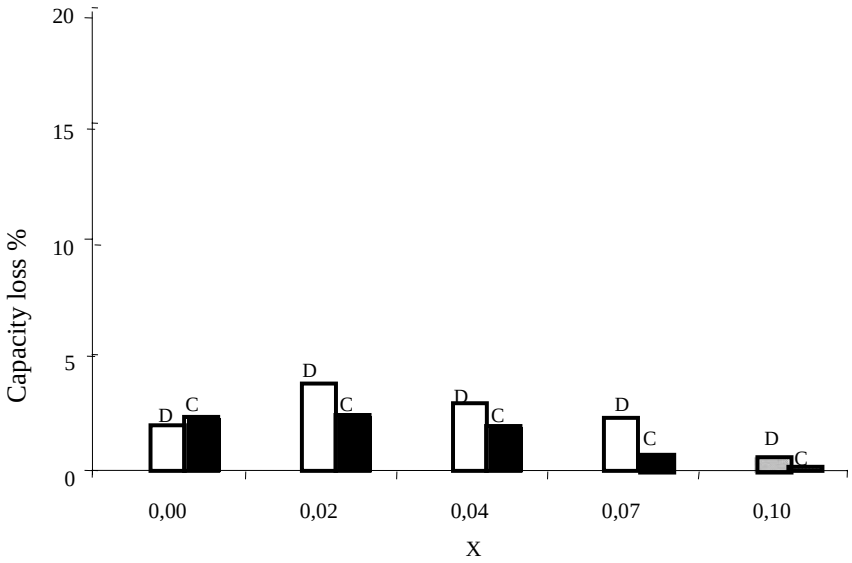

Fig. 5. Capacity loss of $Li[Mn_{1-x}Li_x]O_2$ after 4-week storage in discharged and charged state.

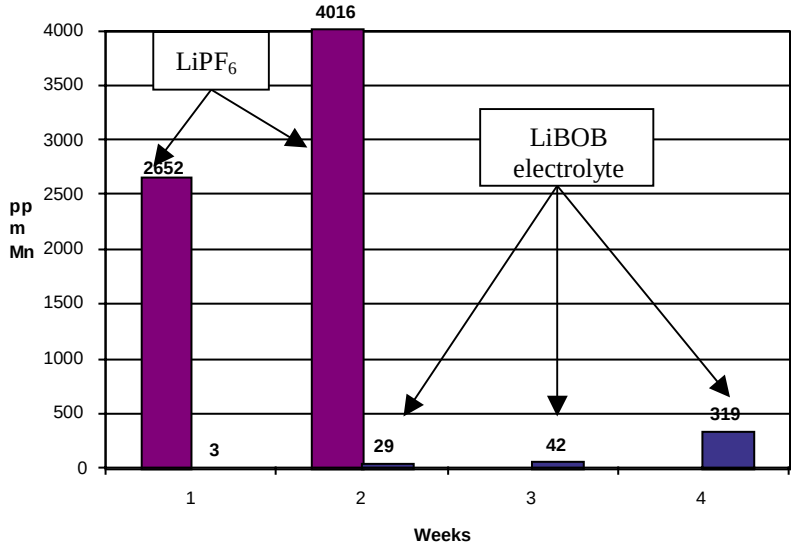

Fig. 6. Dissolution of manganese in $LiPF_6$ and LiBOB containing electrolyte after storage of $LiMn_2O_4$ for different periods at 70 °C.

Therefore, optimized lithium–manganese spinels can exhibit very good cycle life. For nowadays state-of-the-art lithium–manganese spinels, structural changes are no longer the predominant aging mechanisms, as far as reasonable potential windows are chosen.

4.2. Dissolution of manganese in electrolyte

In contrast to lithium–nickel–cobalt oxides, chemical dissolution of lithium–manganese spinel in electrolytes is an existing problem, especially at elevated temperatures [55–66]. The manganese dissolution leads to a loss of active material and therefore capacity fading. Additionally, the precipitation of electronic insulating manganese species, e.g. MnF_2, $MnCO_3$ and various oxides on the cathode has been observed, leading to increasing electrode impedance.

In complete cells, capacity fading is severe and cannot solely be explained by the loss of positive active material. Obviously, dissolved manganese ions move to the negative and are incorporated in the SEI of the carbon electrode. Manganese can be detected on the negative electrode. This leads to electrolyte decomposition and promotes the self-discharge of the lithiated carbon. Therefore, even very small amounts of manganese in the electrolyte affect calendar life of the lithium ion cell.

In general, two different mechanisms of manganese dissolution are discussed:

- Manganese decomposition at low potentials according to: $2Mn(III) \rightarrow Mn(IV) + Mn(II)(solv)$.
- Acid dissolution catalyzed by HF.

The mechanism of acid dissolution is not fully explained yet, but is presumed to evolve qualitatively according to a chemical delithiation reaction scheme: $Li_{1-x}Mn_2O_4 + 2(1-x)HF \rightarrow ((3+x)/4)\lambda\text{-}Mn_2O_4 + (1-x)LiF + (1-x)H_2O + ((1-x)/2)MnF_2$.

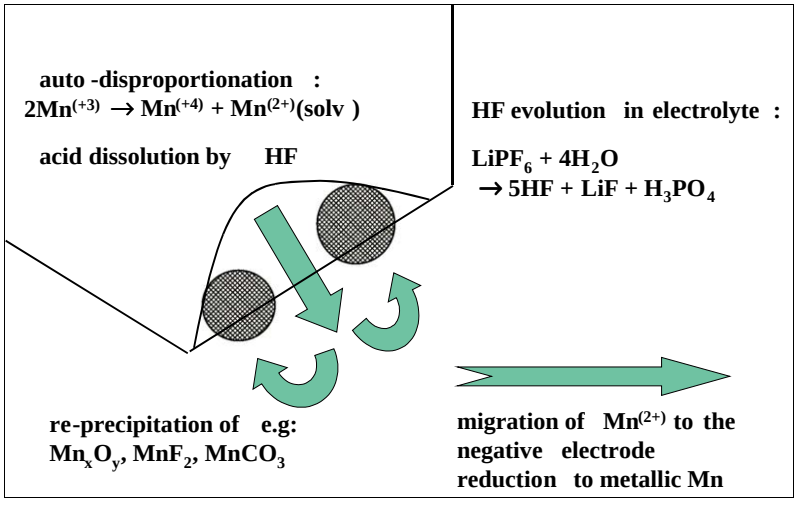

Fig. 7. Schematic description of dissolution mechanisms of lithium–manganese spinel.

Both mechanisms are accelerated at higher temperatures. The decomposition reaction of Mn(III) is predominant in the discharged state, whereas acid dissolution also occurs at higher potentials. Fig. 5 gives the capacity loss of $LiMn_2O_4$ after 4-week storage in the charged and discharged state. It is obvious from this figure that storage in the discharged state is more critical.

Acid dissolution can be minimized by using HF-free conducting salts (Fig. 6). Alternative conductive salts, which are insensitive versus hydrolysis are in development and have promising perspectives. Fig. 7 gives a schematic drawing of manganese dissolution in electrolyte and its impact on the complete cell.

5. Summary

In summary, structural/mechanical capacity fading mechanisms during cycling have been the predominant aging factors for non-optimized cathode materials used in the last decade. In principle, these problems have been overcome by state-of-the-art doped materials.

Al- and Mg-doped lithium–nickel–cobalt oxides exhibit good cycling stability, as far as reasonable potential windows are chosen. According to the relevant phase transitions, for these materials the upper cut-off voltage and the charge rate is more decisive.

Also, lithium-rich or doped lithium–manganese spinels have achieved high cycle numbers. Phase transitions and Jahn–Teller distortion can be suppressed by composition and proper preparation conditions. However, the problem of manganese dissolution in electrolyte has not completely be solved yet. The calendar life of lithium–manganese spinel is dependent on state of charge and temperature. More information is needed in order to understand the interactions of lithium–manganese spinel, electrolyte and negative electrode.

References

[1] P. Arora, R.E. White, M. Doyle, J. Electrochem. Soc. 145 (10) (1998) 3647–3667.
[2] M. Broussely, S. Herreyre, P. Biensan, P. Kasztejna, K. Nechev, R.J. Staniewicz, J. Power Sources 97–98 (2001) 13.
[3] PCT 95/03842.
[4] H. Arai, S. Okada, H. Ohtsuku, M. Ichimura, J. Yamaki, Solid State Ionics 80 (1995) 261.
[5] M. Broussely, F. Perton, J. Labat, R.J. Staniewicz, A. Romero, J. Power Sources 43–44 (1993) 209.
[6] M. Broussely, F. Perton, P. Biensan, J.M. Bodet, J. Labat, A. Lecerf, C. Delmas, A. Rougier, J.P. Peres, J. Power Sources 54 (1995) 109.
[7] J.R. Dahn, U. von Sacken, M.W. Juzkow, H. Al-Janaby, J. Electrochem. Soc. 138 (1991) 2207.
[8] B. Hirano, R. Kanno, Y. Kawamoto, Y. Takeda, K. Yamaura, M. Takano, K. Ohyama, M. Ohashi, Y. Yamaguchi, Solid State Ionics 78 (1995) 123.
[9] A. Hirano, R. Kanno, Y. Kawamoto, K. Oikawa, T. Kamiyama, F. Izumi, Solid State Ionics 86–88 (1996) 791.
[10] E. Levi, M.D. Levi, G. Salitra, D. Aurbach, R. Oesten, U. Heider, L. Heider, Solid State Ionics 126 (1999) 97.
[11] W. Li, J.N. Reimers, J.R. Dahn, Solid State Ionics 67 (1993) 123.
[12] R.V. Moshtev, P. Zlatilova, V. Manev, A. Sato, J. Power Sources 54 (1995) 329.
[13] T. Ohzuku, A. Ueda, M. Nagayam, J. Electrochem. Soc. 140 (1993) 1862.
[14] A. Ueda, T. Ohzuku, J. Electrochem. Soc. 141 (1994) 2010.
[15] T. Ohzuku, A. Ueda, M. Kouguchi, J. Electrochem. Soc. 142 (1995) 4033.
[16] T. Ohzuku, T. Yanagawa, M. Kouguchi, A. Ueda, J. Power Sources 68 (1997) 131.
[17] C. Vogler, B. Löffler, W. Weirather, M. Wohlfahrt-Mehrens, J. Garche, Ionics 8 (2002) 92.
[18] C. Pouillerie, L. Croguennec, P.H. Biensan, P. Willmann, C. Delmas, J. Electrochem. Soc. 147 (2000) 2061.
[19] C.-C. Chang, J.Y. Kim, P.N. Kumta, J. Electrochem Soc. 147 (2000) 1722.
[20] D. Aurbach, B. Markovsky, K. Gamolsky, U. Heider, R. Oesten, Proc. Electrochem. Soc. 99-25 (2000) 233–244.
[21] Y. Kida, A. Kinoshita, K. Yanagida, A. Funahashi, T. Nohma, I. Yonezu, Electrochim. Acta 47 (26) (2002) 4157–4162.
[22] K. Amine, C.H. Chen, J. Liu, M. Hammond, A. Jansen, D. Dees, I. Bloom, D. Vissers, G. Henriksen, J. Power Sources 97–98 (2001) 684–687.
[23] C.H. Chen, J. Liu, K. Amine, J. Power Sources 96 (2) (2001) 321–328.
[24] R.G. Jungst, G. Nagasubramanian, D. Ingersoll, in: Proceedings of the 39th Power Sources Conference, Cherry Hill, USA, 2000, pp. 232–235.
[25] S. Matsuta, Y. Kato, T. Oka, H. Kurokawa, S. Yoshimura, S. Fujitani, J. Electrochem. Soc. 148 (1) (2001) A7–A10.
[26] Y. Wang, X. Guo, S. Greenbaum, J. Liu, K. Amine, Electrochem. Solid State Lett. 4 (6) (2001) A68–A70.
[27] D. Zhang, B.S. Haran, A. Durairajan, R.E. White, Y. Podrazhansky, B.N. Popov, J. Power Sources 91 (2) (2000) 122–129.
[28] R.J. Gummow, A. de Kock, M.M. Thackeray, Solid State Ionics 69 (1994) 59–67.
[29] M.M. Thackeray, Y. Shao-Horn, A.J. Kahaian, Electrochem. Solid State Lett. 1 (1998) 7–9.
[30] D.H. Jang, J.S. Young, S.M. Oh, J. Electrochem. Soc. 143 (1996) 2204–2211.
[31] Y. Gao, J.R. Dahn, Solid State Ionics 84 (1996) 33–40.
[32] Y. Xia, Y. Zhou, M. Yoshio, J. Electrochem. Soc. 144 (1997) 2593–2600.
[33] J.M. Tarascon, W.R. McKinnon, F. Coowar, et al., J. Electrochem. Soc. 141 (1994) 1421–1431.
[34] T. Ohzuku, M. Kitigawa, T. Hirai, J. Electrochem. Soc. 137 (1990) 769.
[35] Y. Xia, M. Yoshio, J. Electrochem. Soc. 143 (1996) 825.
[36] W. Liu, K. Kowal, G.C. Farrington, J. Electrochem. Soc. 145 (1998) 559.
[37] M.N. Richard, I. Koetschau, J.R. Dahn, J. Electrochem. Soc. 144 (1997) 554.
[38] S. Mukerjee, T.R. Thurston, N.M. Jisrawi, X.Q. Yang, J. McBreen, M.L. Daroux, X.K. Xing, J. Electrochem. Soc. 145 (1998) 466.
[39] M.R. Palacin, Y. Chabre, L. Dupont, M. Hervieu, P. Strobel, G. Rousse, C. Masquelier, M. Anne, G.G. Amatucci, J.-M. Tarascon, J. Electrochem. Soc. 147 (2000) 845.
[40] M.R. Palacin, G. Rousse, M. Morcrette, L. Dupont, C. Masquelier, Y. Chabre, M. Hervieu, J.-M. Tarascon, J. Power Sources 97–98 (2001) 398–401.
[41] M.R. Palacin, G.G. Amatucci, M. Anne, Y. Chabre, L. Seguin, P. Strobel, J.M. Tarascon, G. Vaughan, J. Power Sources 81–82 (1999) 627–631.
[42] Y. Shin, A. Manthiram, Abstracts of Fall Meeting, Electrochemical Society, Salt Lake City, USA, October 2002.

[43] Y. Gao, J.R. Dahn, Solid State Ionics 84 (1–2) (1996) 33–40.
[44] M. Wohlfahrt-Mehrens, A. Butz, R. Oesten, J. Power Sources 68 (1997) 582–585.
[45] A.D. Robertson, S.H. Lu, W.F. Howard, J. Electrochem. Soc. 144 (1997) 3500–3512.
[46] J.M. Tarascon, E. Wang, F.K. Shokoohi, et al., Electrochem. Soc. 138 (1991) 2859–2864.
[47] B. Banov, Y. Todorov, A. Trifonova, A. Momchilov, V. Manev, J. Power Sources 68 (1997) 578–581.
[48] Y. Chida, H. Wada, K. Shizuka, J. Power Sources 81–82 (1999) 454–457.
[49] H. Huang, C.A. Vincent, P.G. Bruce, J. Electrochem. Soc. 146 (10) (1999) 3649–3654.
[50] J.M. Tarascon, F. Coowar, G. Amatuci, F.K. Shokoohi, D.G. Guyomard, J. Power Sources 54 (1) (1995) 103–108.
[51] Y. Xia, Y.H. Zhou, M. Yoshio, J. Electrochem. Soc. 144 (8) (1997) 2593–2600.
[52] B. Banov, Y. Todorov, A. Trifonova, A. Momchilov, V. Manev, J. Power Sources 68 (1997) 578–581.
[53] Y. Xia, M. Yoshio, J. Electrochem. Soc. 144 (1997) 4186–4194.
[54] Y. Gao, J.R. Dahn, J. Electrochem. Soc. 143 (1996) 100–114.
[55] T. Aoshima, K. Okahara, C. Kiyohara, K. Shizuka, J. Power Sources 97–98 (2001) 377–380.
[56] D. Aurbach, M.D. Levi, K. Gamulski, B. Markovsky, G. Salitra, E. Levi, U. Heider, L. Heider, J. Power Sources 82 (1999) 472–479.
[57] Y. Chen, Y. Zhao, C. Du, Q. Liu, Dianchi 31 (2) (2001) 75–77.
[58] Z.Y. Chen, X.Q. Liu, L.Z. Gao, Z.L. Yu, Chin. J. Inorg. Chem. 17 (3) (2001) 325–330.
[59] Y. Chen, Q. Liu, Dianchi 31 (4) (2001) 198–201.
[60] J. Cho, G.B. Kim, H.S. Lim, C.-S. Kim, S.-I. Yoo, Electrochem. Solid State Lett. 2 (1999) 607.
[61] A. Du Pasquier, A. Blyr, A. Cressent, C. Lenain, G. Amatucci, J.M. Tarascon, J. Power Sources 82 (1999) 54–59.
[62] B.S. Haran, A. Durairajan, P. Ramadass, R.E. White, B.N. Popov, in: Proceedings of the 36th Intersociety Energy Conversion Engineering Conference, Savannah, USA, vol. 2, 2001, pp. 935–940.
[63] E. Iwata, K.-I. Takahashi, K. Maeda, T. Mouri, J. Power Sources 81–82 (1999) 430–433.
[64] S. Komaba, N. Kumagai, T. Sasaki, Y. Miki, Electrochemistry (Tokyo) 69 (10) (2001) 784–787.
[65] H. Oka, S. Kasahara, T. Okada, E. Iwata, M. Okada, T. Shoji, H. Ohki, T. Okuda, Solid State Ionics 144 (1–2) (2001) 19–29.
[66] H. Yamane, T. Inoue, M. Fujita, M. Sano, J. Power Sources 99 (1–2) (2001) 60–65.